Prediction of Interface Dielectric Relaxations in Bimodal Brush Functionalized Epoxy Nanodielectrics by Finite Element Analysis Method

Yanhui Huang, Timothy M. Krentz, J. Keith Nelson,
and Linda S. Schadler
Dept. of Material Science and Engineering
Rensselaer Polytechnic Institute
Troy, NY USA

Yang Li, He Zhao, and L. Catherine Brinson
Dept. of Material Science and Engineering
University of Northwestern
Evanston, IL USA

Michael Bell and Brian Benicewicz
Dept. of Chemistry and Biochemistry
University of South Carolina
Columbia, SC USA

Ke Wu and Curt M. Breneman
Dept. of Chemistry and Chemical Biology
Rensselaer Polytechnic Institute
Troy, NY USA

***Abstract*- Finite element 2-D analysis was implemented to simulate the dielectric spectra of nanodielectrics. As a test case, silica modified with a high graft density of short molecules and a low graft density of epoxy compatible chains were incorporated into epoxy. TEM images of the composites filler distribution were used to construct the model geometry with the interfacial area specifically included. The interfacial area was found to have dielectric relaxation behavior different from that of the matrix, as described by additional fitting parameters. This modeling method has the potential to improve our understanding of the impact of interface properties on the dielectric properties of composites.**

I. INTRODUCTION

Polymer nanodielectrics are of interest because the properties can be tuned via filler interface modification and filler dispersion [1]. Accurately predicting the dielectric properties has proven to be difficult. Research has demonstrated the importance of the filler / matrix interfacial region in controlling the bulk properties [2]. Filler / matrix interactions can either enhance or restrict the mobility of polymer chains in the interfacial region and thus alter the relaxation times [3]. Building on traditional mixing rules for a simple two-phase system, Todd and Shi [1] developed a theoretical model to account for contributions from the interfacial region. Though providing a more precise approach, this model does not consider the explicit geometry and dispersion of filler in the matrix, thus limiting its accuracy for systems that do not have uniform or random filler distribution. Moreover, predicting the dielectric properties over a range of frequencies is critical because many electronic devices operate over a wide range of frequencies. However, no current models have yet taken this into account.

Our previous work [4] showed that the use of two populations of molecules (a bimodal brush – see Figure 1) on a nanosilica particle surface could ensure good filler dispersion and improve the breakdown strength up to 40 %; 1. a high graft density of short molecules that have potential electron trapping states - such as ferrocene and terthiophene, and 2. a low graft density of matrix compatible long molecules poly(glycidyl methacrylate) (PGMA). In this paper, we explore the use of finite element analysis (FEA) to analyze experimental dielectric spectroscopy data and predict the properties of the interfacial area in the polymer. From TEM images, realistic nanoparticle dispersions are captured in the FEA and the interfacial region is explicitly included. By fitting the experimental dielectric spectroscopy data using a superposition of Debye functions [5], the continuous dielectric spectroscopy of polymer matrix was obtained and used as input to the simulation. The relaxation behavior of the interfacial region was obtained by matching the simulation results with the experimental data of the composite. It was found that the relaxation of the interfacial region can be expressed in the same form as the matrix but with additional tuning parameters, each with physical meaning. This approach can be used to provide significant insight into the impact of surface ligand chemistry on the interface dielectric properties and thus serves as a preliminary step in an effort to permit more meaningful modeling in nanodielectrics.

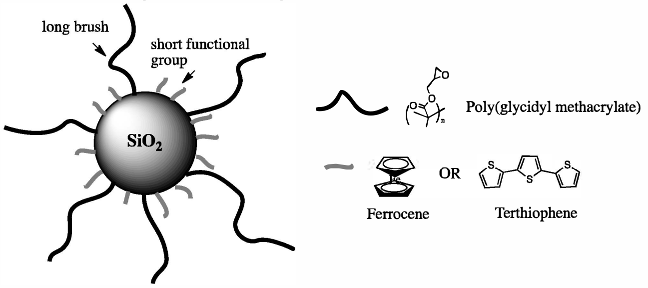

Fig. 1. Bimodal brush functionalized silica nanoparticle

978-1-4799-7525-9/14/$31.00 @2014 IEEE

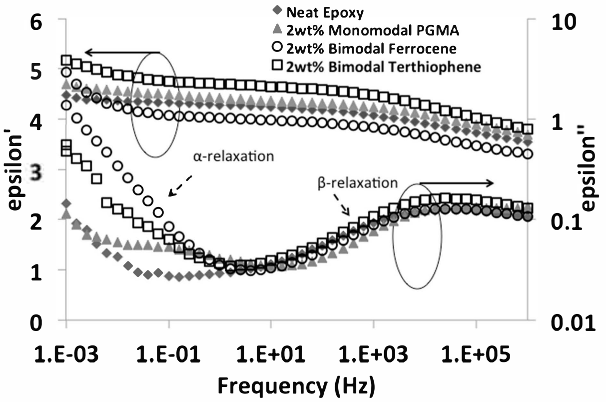

Fig. 2. Dielectric spectroscopy of bimodal brush functionalized epoxy nanodielectrics.

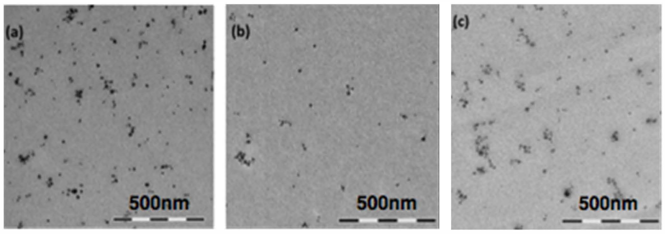

Fig. 3. TEM images of bimodal brush functionalized epoxy nanocomposite. (a) monomodal PGMA, (b) biomodal ferrocene, (c) bimodal terthiophene.

II. EXPERIMENTAL METHODS

A. *Experimental Data*

Our previous work showed that bimodal brush functionalized epoxy nanodielectrics exhibit dielectric properties that depend on the surface chemistry of the silica nanoparticle [4]. Finite element analysis was implemented based on the experimental dielectric spectra (Figure 2) and TEM images (Figure 3). The increase in dielectric loss at low frequency is due to the alpha relaxation caused by polymer backbone chain motion, while the peak shown around 10^4 Hz is due to beta relaxation caused by side chain crankshaft motion. To simulate any potential interfacial polarization, the DC conductivity of the matrix and interfacial region was input as 10^{-15} S/m.

B. *Finite Element Simulation of Dielectric Spectroscopy*

A two dimensional finite element model was built in the commercial software package COMSOL to simulate the composite dielectric spectroscopy. One advantage of FEA compared to homogenization models is the ability to model the composite morphology explicitly. The FEA simulation took in filler and matrix properties as input and provided frequency-dependent complex permittivity of the composites.

a) Microstructure characterization

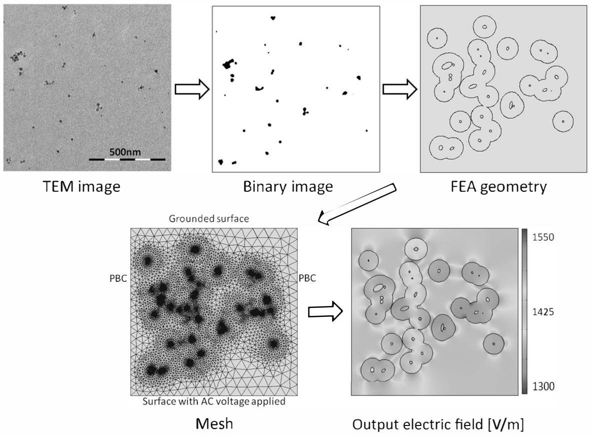

Fig. 4. A schematic of microstructure characterization process. The physical dimension of the image is 1.1μm. An SVE structure was cut from the original TEM image of 2wt% bimodal ferrocene silica filled epoxy. An FEA mesh was generated along with characterization algorithms in COMSOL.

The geometry of the nanocomposites was obtained from descriptor-based TEM image characterization (two point correlation functions) that generates the explicit morphology of all three constituents: nanofiller, matrix and matrix-filler interface. Gray scale TEM images were first transformed into binary images [6]. A transformation algorithm was used to determine the TEM gray scale pixel threshold to distinguish between matrix and fillers and generate a binary filler-matrix microstructure. For simplicity, nanofillers were characterized as ellipses with the same area as clusters of black pixels in the TEM images. This characterization process ensured that the volume fraction (VF) of nanofiller used in the FEA model was consistent with the corresponding experimental value. The matrix-filler interfacial region was represented by a single phase with uniform thickness surrounding the nanofillers. The thickness of this region was assumed to be 60 nm, the details of which will be discussed in section c).

b) Configuration of the model

The morphology of the fillers with the same descriptors as captured from TEM images was built in COMSOL as a statistical volume element (SVE). The schematic of the model and the mesh are shown in Figure 4. Triangular elements were used to capture the shape of the features with a refined mesh in the interfacial region. Periodic boundary conditions were configured at the lateral surfaces. AC voltage was applied at the bottom of the sample with the frequency sweep from 10^{-3} Hz to 10^6 Hz and the top was grounded. The structure was regarded as a parallel plate capacitor. The effective dielectric constant of the composites was calculated using the following equation:

$$\varepsilon_r(\omega) = \frac{J_y^*(\omega)d}{j\omega V^*(\omega)\varepsilon_0} \tag{1}$$

Here $V^*(\omega)$ is the applied voltage as a function of angular frequency ω, and $J_y^*(\omega)$ is the average complex AC current density along the direction perpendicular to the electrode and was measured at the grounded surface from the simulation output. d is the sample thickness, and ε_0 is the vacuum permittivity as 8.85×10^{-12} F/m.

c) Modeling broadband dielectric spectroscopy using a superposition of Debye functions

Due to the inherent structural heterogeneity in polymers, broadened relaxation processes are observed, which can be formally described by a superposition of independent Debye functions with different relaxation times [5]:

$$\varepsilon'(\omega) = \varepsilon_\infty + \sum_{i=1}^{n} \frac{\Delta\varepsilon_i}{1+(\omega\tau_i)^2} \tag{2}$$

$$\varepsilon''(\omega) = \sum_{i=1}^{n} \frac{\Delta\varepsilon_i \omega\tau_i}{1+(\omega\tau_i)^2} \tag{3}$$

$\varepsilon'(\omega)$ and $\varepsilon''(\omega)$ represent the real and imaginary parts of the permittivity and n was taken as 25 to accurately capture the shape of the curve. $\Delta\varepsilon_i$ and τ_i are the dielectric relaxation intensity and relaxation time for each Debye component; ε_∞ is the real permittivity at the maximum frequency. $\Delta\varepsilon_i, \tau_i$ and ε_∞ are obtained through fitting the experimental spectroscopy of the matrix to the form in (2) and (3) using the algorithm for a Prony series presented in [7], which allows simultaneous fitting of the real and imaginary parts. At each tested frequency, the values of the real and imaginary parts of the neat epoxy were modeled and taken as the properties of the matrix in the FEA. The permittivity of silica fillers was taken as a frequency independent constant of 3.9 and the DC conductivity was taken as 10^{-18} S/m [8].

One of the core features was the consideration of the interfacial area. Based on discussions in [1][9] and previous studies on viscoelasticity [3], the thickness was estimated as 60 nm. The relaxation behavior of the interfacial region was expressed as a superposition of Debye functions, which originated from the matrix but with additional tuning parameters:

$$\varepsilon'_{int}(\omega) = \varepsilon_\infty + c + M_\alpha \sum_{\tau_i>\tau_0} \frac{\Delta\varepsilon_i}{1+(S_\alpha\omega\tau_i)^2} + M_\beta \sum_{\tau_i<\tau_0} \frac{\Delta\varepsilon_i}{1+\left(S_\beta\omega\tau_i\right)^2} \tag{4}$$

$$\varepsilon''_{int}(\omega) = M_\alpha \sum_{\tau_i>\tau_0} \frac{S_\alpha\Delta\varepsilon_i\omega\tau_i}{1+(S_\alpha\omega\tau_i)^2} + M_\beta \sum_{\tau_i<\tau_0} \frac{S_\beta\Delta\varepsilon_i\omega\tau_i}{1+\left(S_\beta\omega\tau_i\right)^2} \tag{5}$$

The α and β relaxations were modeled separately. Terms with τ_i greater than τ_0 were modeled as α relaxation while those with τ_i smaller than τ_0 were modeled as β relaxation. Here we take $\tau_0 = 1$ sec. *M, S* and *c* are tuning parameters with a subscript of the corresponding relaxation. The parameters were obtained by matching the simulation output to the experiment data. The whole modeling procedure was combined in a Matlab script for automatic processing.

TABLE I. THE TUNING PARAMETERS FOR THE PROPERTIES OF THE INTERFACIAL AREA

Sample	S_α	M_α	S_β	M_β	*c*
Monomodal PGMA	4.0	3.0	0.25	1.2	0.4
Bimodal Ferrocene	0.05	4.0	0.75	1.1	-0.7
Bimodal Terthiophene	0.02	0.5	0.75	1.8	0.6

III. RESULTS AND DISCUSSION

A. *Prediction of Interfacial Dielectric Relaxation*

In practice the following strategy was employed to tune the parameters in (4) and (5). First, the interfacial region in the FEA model was not included, and the loss peak in the spectra of ε" from the simulation was compared with the experimental data of the composites. Then the interfacial area was activated and the S_α and S_β were adjusted so that the loss peaks matched the experimental data by frequency. Next the M_α and M_β were tuned to adjust the shape of ε". Finally ε' was compared and suitable adjustment was made to the additional constant *c*.

The value of the parameters after tuning is shown in Table I. A comparison of the spectra from modeling and experiments is shown in Figure 5, with the 2wt% bimodal terthiophene silica filled epoxy taken as an example. The calculated spectra of the interfacial region are also shown in Figure 5.

Figure 5 indicates that the configuration of the interfacial area was essential in the modeling. A significant deviation of simulated results from experimental data can be observed if the model is only composed of filler and matrix without interfacial area (open triangle in Figure 5). Similarly, a geometry with highly clustered nanofillers will not show as much deviation from the matrix properties.

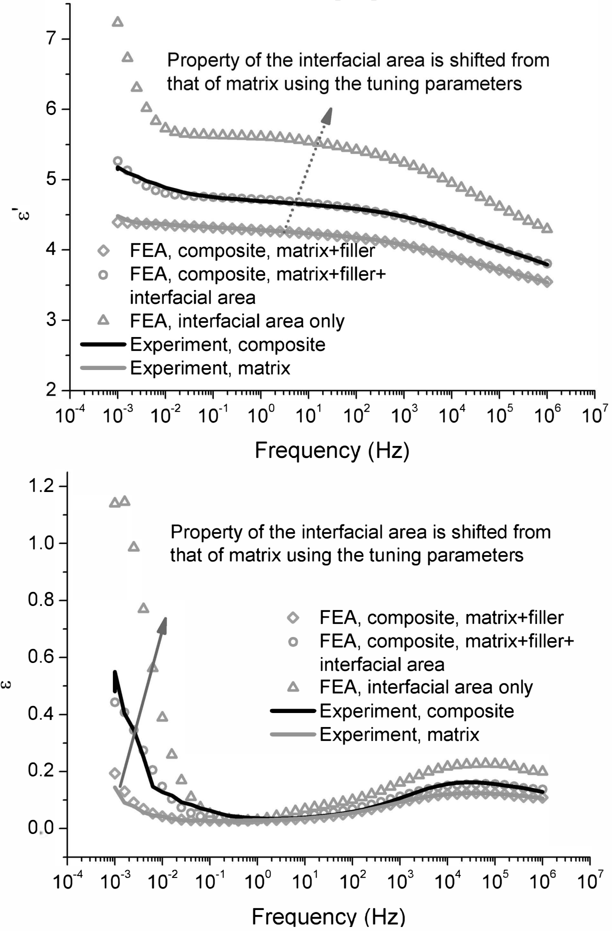

Fig. 5. The comparison between the experimental data and the simulated dielectric spectroscopy with and without interfacial area for 2wt% bimodal terthiophene silica filled epoxy.

The properties of the interfacial region were influenced by the short molecules. The interfacial relaxation behavior is reflected in the five tuning parameters in (4) and (5). S_α and S_β, which account for the frequency shift of the curve, reflect the change in α and β relaxation times of the interfacial area. M_α and M_β, which describe the vertical shift of the curve, reflect the change in the extent of polarization. The tuning parameter c reflects the change in permittivity beyond 10^6 Hz where dipolar, ionic and electronic polarizations contribute. For the system tested, S was typically smaller than one and M was larger than one, indicating that the chains at the interface experienced greater mobility and enhanced polarizability compared to the bulk matrix. One exception was the monomodal PGMA system with a S_α of 4.0. This is due to the relatively poor fitting of the loss curve. Because the curve has a dissimilar shape compared to the matrix, using only two parameters to simply shift and stretch the curve may not be sufficient to accurately capture the shape difference. More parameters are needed to improve the fitting. The parameter c shows more significant change as the short functional group was introduced to the nanoparticle surface. Considering that the volume fraction of these functional groups is less than 0.01 % in both systems, and the dielectric constants are less than 10 [10], the polarization of these molecules is not the cause for the large change in the dielectric spectra. The difference is potentially due to the change in polarizability of polymers in the interfacial region as a result of interaction with the short molecules. Ferrocene and terthiophene have opposite effects on the local polarizability: ferrocene tends to depress (gives negative c) while terthiophene tends to enhance (gives a positive c). But unfortunately the simulation of this phenomenon is beyond the capability of FEA. Further molecular level simulation is required to provide a microscopic understanding of the phenomenon.

B. Modeling Low Frequency Behavior

The increase in dielectric loss below 1 Hz can be caused by several mechanisms other than α-relaxation, including electronic DC conduction [5], Quasi-DC processes [11], and interfacial polarization [5]. The volume DC conductivity was measured using a guarded-electrode system under the field of 2 kV/mm from the steady state current. It gives approximately the same value of 1.5×10^{-15} S/m ($\pm6\times10^{-16}$ S/m) for each system.

From $\varepsilon''(\omega) = \sigma_0/\varepsilon_0\omega$, the ε'' arising from DC conduction is less than 0.04 at 10^{-3} Hz, which contributes no more than 40% of the loss in each system. Since the dielectric spectrometer operates at a low voltage of 1 V and the DC conductivity of insulating polymers is highly field dependent, the real DC conduction reflected in the spectroscopy is almost negligible.

In Quasi-DC conduction dominated phenomenon, the dielectric constant and loss usually follow the same power law behavior and thus the $\tan\,\delta$ is constant over the frequency range, which is not observed in our measurement.

Interfacial polarization, which arises from the blocked space charges at an internal phase boundary, is automatically solved by COMSOL in the process of satisfying boundary conditions from the input of the conductivity and permittivity of each phase. A rough calculation using a simple triple layer model shows that the relaxation times of interfacial polarizations are around 10^5 seconds. Even though we cannot see the complete loss peak in the spectra, the rising part of it was still included in the simulation.

IV. CONCLUSIONS

The dielectric spectroscopy of bimodal brush functionalized epoxy nanodielectrics can be successfully simulated by FEA based on the geometry of filler distribution with interfacial area included. The relaxation behavior of the matrix was described with a superposition of Debye functions, and that of the interfacial area was obtained by adjusting additional tuning parameters in the matrix formula. Based on analysis of the tuning parameters, the interfacial area in our composites is likely to have an increased chain mobility and polarizability in the measured frequency range. And the change of polarization at higher frequencies is possibly due to the short functional groups like terthiophene and ferrocene. Future work will focus on improving the accuracy of fitting and expanding the simulation to 3-D systems.

ACKNOWLEDGMENT

This work is supported by Nanoscale Science and Engineering Center for Directed Assembly of Nanostuctures and the U.S. Office of Naval Research under Grant N000141310173.

REFERENCES

[1] J. K. Nelson, *Dielectric Polymer Nanocomposites*: Springer, 2009.

[2] M. Roy, J. Nelson, R. MacCrone, L. Schadler, C. Reed, and R. Keefe, "Polymer Nanocomposite Dielectrics-the Role of the Interface," *Dielectrics and Electrical Insulation, IEEE Transactions on,* vol. 12, pp. 629-643, 2005.

[3] C. M. Breneman, L. C. Brinson, L. S. Schadler, B. Natarajan, M. Krein, K. Wu, et al., "Stalking the Materials Genome: A Data-Driven Approach to the Virtual Design of Nanostructured Polymers," Advanced Functional Materials, vol. 23, pp. 5746-5752, Dec 10 2013.

[4] S. Virtanen, T. M. Krentz, J. K. Nelson, L. S. Schadler, M. Bell, B. Benicewicz, *et al.*, "Dielectric Breakdown Strength of Epoxy Bimodal-Polymer-Brush-Grafted Core Functionalized Silica Nanocomposites," *Dielectrics and Electrical Insulation, IEEE Transactions on,* vol. 21, pp. 563-570, 2014.

[5] F. Kremer and A. Schönhals, *Broadband dielectric spectroscopy*: Springer, 2003.

[6] H. Xu, Y. Li, C. Brinson, and W. Chen, "A Descriptor-Based Design Methodology for Developing Heterogeneous Microstructural Materials System," Journal of Mechanical Design, vol. 136, 2014.

[7] R. D. Bradshaw and L. C. Brinson, "Physical Aging in Polymers and Polymer Composites: An Analysis and Method for Time-Aging Time Superposition," *Polymer Engineering and Science,* vol. 37, pp. 31-44, Jan 1997.

[8] P. R. Gray and R. G. Meyer, *Analysis and Design of Analog Integrated Circuits*: John Wiley & Sons, Inc., 1990.

[9] T. Tanaka, M. Kozako, N. Fuse, and Y. Ohki, "Proposal of a Multi-Core Model for Polymer Nanocomposite Dielectrics," Dielectrics and Electrical Insulation, IEEE Transactions on, vol. 12, pp. 669-681, 2005.

[10] M. Okutan, Y. Yerli, S. E. San, F. Yılmaz, O. Günaydın, and M. Durak, "Dielectric Properties of Thiophene Based Conducting Polymers," Synthetic metals, vol. 157, pp. 368-373, 2007.

[11] D. K. Das-Gupta, "Conduction Mechanisms and High-Field Effects in Synthetic Insulating Polymers," *Dielectrics and Electrical Insulation, IEEE Transactions on,* vol. 4, pp. 149-156, 1997.